Experimental and CFD Study of Flow Phenomenon in Flowrate-amplified Flotation Element

Wang Xinzhe

The State Key Lab of Fluid Power Transmission and Control, Zhejiang University, Zheda Road 38, 310027 Hangzhou, China, E-Mail: wanghsinche@hotmail.com

Professor Dr.-Ing. Li Xin

The State Key Lab of Fluid Power Transmission and Control, Zhejiang University, Zheda Road 38, 310027 Hangzhou, China, E-Mail: vortexdoctor@zju.edu.cn

Abstract

Focusing on reducing the air consumption of an air flotation rail system, a flowrate-amplified flotation element was recently developed. This new flotation element ulitises the rotational flow to intake extra air via an intake hole, and thus, effectively improves the flotation height. Compared to a conventional flotation element, the flowrate-amplified flotation element can reduce air consumption by approximately 50% for the same load and flotation height. To gain an understanding of the flow phenomenon in the flowrate-amplified flotation element, experiments and CFD simulations are conducted in this study. Based on the results, we found that the flowrate-amplified flotation element could take a part of the kinetic energy of the rotating air to suck in extra air. The intake hole greatly affects the pressure field and velocity field of the flotation element. Additionally, the effects of the variant gap height and supplied flow rate were also discussed. The results indicate that the pressure distribution decreases as the gap height increases and increases as the supplied flow rate increases.

KEYWORDS: air flotation; air intake; rotational flow; glass substrate; CFD

1. Introduction

In the manufacturing and detection procedures for large-scale glass substrates for liquid crystal displays, the workpiece needs to be transported repeatedly between different workbenches. Since glass substrates become larger but thinner (the dimensions of a 10th generation glass substrate are above 2850 mm × 3050 mm, while its thickness is only 0.7 mm), a slight local stress concentration will cause severe deformation and scratches /1/. In this case, traditional contact transmission methods (such as using roller or belt conveyor systems) are not suitable anymore. In the modern glass industry, an air

flotation rail system, as shown in **Figure 1**, is usually used to transport glass substrates without contact /1,2/. Because the glass substrates float on the flotation plane, using an air flotation rail system can decrease most of the damage caused by contact and increase the workpiece transmission speed between workbenches.

As the primary components of an air flotation rail system, numerous flotation elements are distributed on the rail plane. When pressurized air is supplied, a thin air film that develops between the workpiece and flotation plane can suspend the glass substrates over the rail. However, conventional air flotation elements have some disadvantages, such as uneven pressure distribution, local stress concentration, and high maintenance costs /3-5/. Additionally, the non-contact transportation of large-scale glass substrates consumes a lot of highly clean pressurized air. Therefore, the means of reducing the air consumption while producing a uniform pressure distribution becomes a major technical concern.

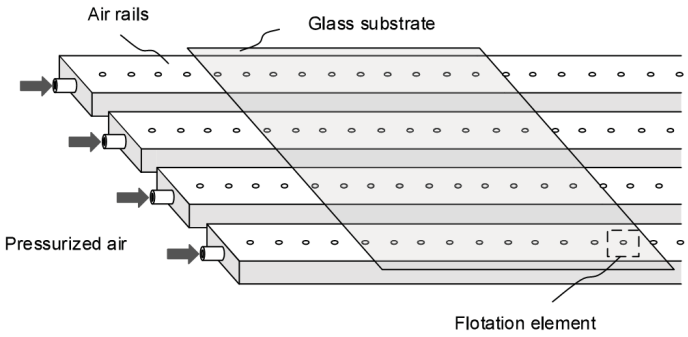

Figure 1: Air flotation rail system for large scale glass substrate

In a previous study, we proposed a new flotation element that can intake extra air. This element was called the flowrate-amplified flotation element and it is shown in **Figure 2** /6/. It consists of a flotation plane, a chamber, an intake hole, and two nozzles in the tangential direction of the chamber wall. When the pressurized air is ejected from the nozzles, a high-speed rotational flow develops in the chamber and produces negative pressure owing to centrifugal force. Because of the pressure difference between the centre of chamber and the atmosphere, extra air is sucked into the chamber through the intake hole. Then, the extra air and supplied air are mixed and they flow together into the gap between the workpiece and flotation plane (abbreviated as ‘the gap’ in the following sections) to form an air film. Our previous study found that, compared to a conventional orifice flotation element, this new design can reduce air consumption by approximately 50% for the same load and flotation height.

In the following sections, we will measure the pressure distributions and conduct a series of CFD simulations to investigate the flow phenomenon in the new flotation element. Additionally, we will discuss its characteristics for different flotation heights and supplied flow rates.

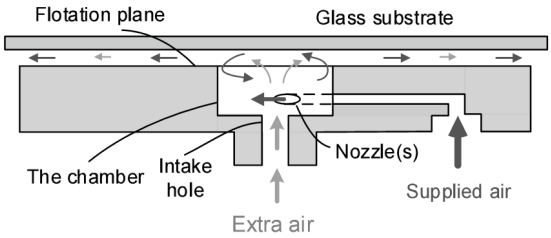

Figure 2: Schematic of flowrate-amplified flotation element

2. Experimental and Numerical Methods

The overall pressure and flow rate data are necessary for studying the flow phenomenon of a flotation element. Since obtaining the data inside the flotation element directly by an experimental method may not be practical, this paper will combine experiments and CFD simulations to investigate the flow phenomenon. First, an apparatus is built to measure the pressure distribution of the gap under different work conditions. Second, corresponding CFD models are designed to simulate the flow field of the flotation element and are verified by experimental data. In this way, the overall pressure and flow rate data can be obtained.

2.1. Experimental setup to measure pressure distribution

The flowrate-amplifier flotation element used in the experiment is shown in **Figure 3** and its essential parameters are listed in **Table 1**. To get the pressure distribution of the gap**,** we design a pressure measurement apparatus, as shown in **Figure 4**. It consists of a movable frame, a fixed support, a precision plane, a pressure sensor, and some necessary circuits. The flotation element fixed in a movable frame is parallel to the precision plane. Three pins located in the movable frame keep the flotation element's work surface and precision plane at constant distance during the experiment process. The movable frame, restricted in the fixed support by pins, has three degrees of freedom. It can move along the Z-axis, as well as rotate around the X and Y-axes. To collect the pressure signal, a pressure sensor is connected to the pressure tap that is located at the centre of the precision plane through the tube. In this way, the pressure distribution can be measured by continuously recording the pressure while the step motor is running at a slow speed.

It is worth noting that the gap height is set very carefully using the following steps. First, ensure the work surface of flotation element is in full contact with the precision plane; second, place shims between the work surface and the precision plane and set the pins until their tips touch the top of the flotation element; finally, turn the pin clamps tightly, and take the shims out of the gap. In this way, the height of the gap is set.

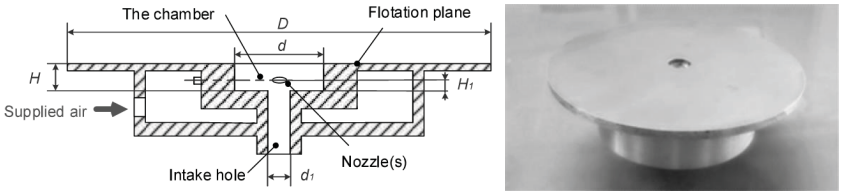

Figure 3: Structure and photograph of flowrate-amplified flotation element

D	d	d_1	H	H_1
90	8	2	2.5	1

Table 1: Size of structure parameters (Unit: mm)

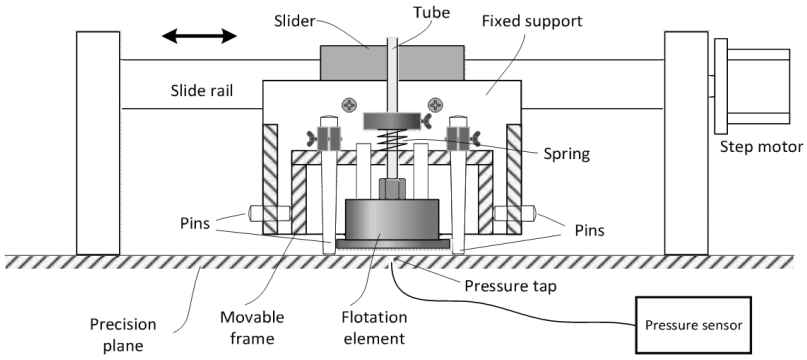

Figure 4: Schematic of pressure measurement apparatus

2.2. CFD simulation method

The mesh for the CFD simulation includes air film, nozzles, an intake hole and an atmosphere. Since the boundary conditions of the air film and intake hole are too complicated to set directly, expanding the calculation field that is near air film and intake hole is necessary to improve the accuracy of the simulation. Therefore, the mesh is divided into several parts: (i) the parts of the air film, intake hole, and nearby atmosphere which are meshed with hexahedral mesh; and (ii) the part of the chamber and nozzles, which is meshed with tetrahedral mesh. The total number of cells is more than 1.8 million and the cell quality is above 0.3.

The nozzles are set as mass flow inlet. As the calculation field is expanded, it is rational to regard the pressure of atmosphere around the flotation element as atmospheric pressure, and set its boundary condition as pressure outlet. Similarly, the calculation field near the intake hole is large enough to set its boundary condition as a pressure inlet with zero gauge pressure. In this study, a swirling flow dominant RNG k-ε turbulence model is applied with enhanced near wall treatment.

3. Results and Discussion

3.1. Verification of simulation result

The simulation results need to be verified by the experimental data. In previous work, the intake flow rate at various gap heights was measured /6/. Hence, we set the supplied flow rate to 2 L/min (ARN) and simulated the model with respective gap heights of 0.25 mm, 0.30 mm, 0.35 mm, and 0.40 mm. The data for the intake flow rate are presented in **Figure 5**, where the solid line represents the experimental results of previous work and the dashed line represents simulation results calculated by CFD. The trends of two lines are very similar: both of them increase sharply at first, reach a peak when the gap height is 0.35 mm, and then fall off. As **Table 3** shows, every single model's CFD simulation result is coincident with its experimental result.

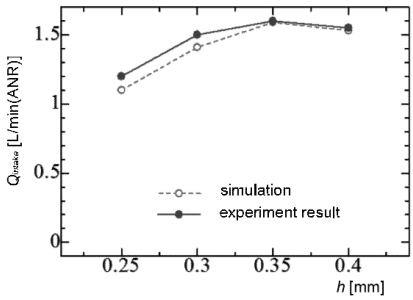

Figure 5: Intake flow rate

h [mm]	$Q_{intake,exp}$ [L/min]	$Q_{intake,CFD}$ [L/min]	$Q_{intake,CFD}$ / $Q_{intake,exp}$ [-]
0.25	1.20	1.100	91.65%
0.30	1.50	1.406	93.74%
0.35	1.60	1.592	99.48%
0.40	1.55	1.527	98.50%

Table 3: Comparison of experimental and CFD intake flow rate

The pressure distribution of the gap is another primary characteristic of the flotation element. The radial direction pressure distribution with a supplied flow rate of 2 L/min(ARN) and a gap height of 0.25 mm was measured by the pressure measurement apparatus. The experimental data is compared with the CFD results, as shown in **Figure 6**. It is clear that the difference between the CFD results and experimental data is quite small. In addition, the pressure peaks that appear at the edge and centre of chamber can be reflected well in CFD. Even when the intake hole is closed, as shown at the right of Figure 6, the pressure data of CFD is quite close to the experimental data.

Hence, it can be said that CFD simulations closely reproduced the flow phenomenon inside the chamber, and that the simulation results are credible.

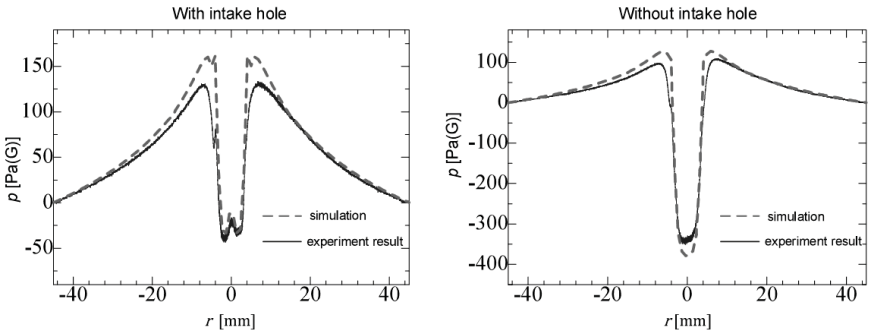

Figure 6: Pressure distribution in the gap between workpiece and flotation plane

3.2. Flow phenomenon inside the chamber

First, the flow phenomenon inside the chamber is investigated. In order to study how the intake hole influences the flow field of the chamber, flotation element models with and without an intake hole were simulated with same supplied flow rate and gap height. The velocity contours and vectors in the $\vec{z}$ direction are presented in **Figure 7**.

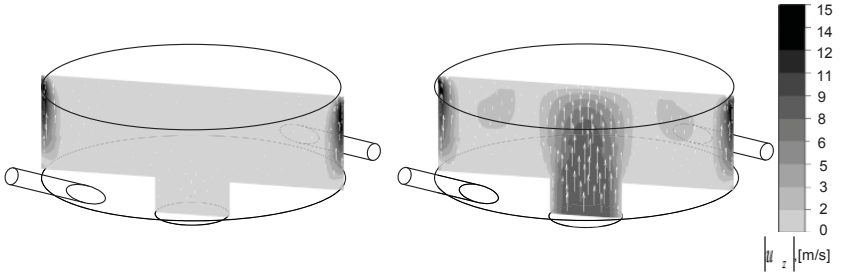

Figure 7: Velocity contour and vectors in $\vec{z}$ direction (left: flotation element without intake hole, right: flotation element with intake hole)

It is obvious that the vertical velocity of air inside the flotation element without the intake hole is quite low, while the velocity is much higher at the centre of the flotation element with the intake hole. The CFD results indicate that the intake hole significantly influences the flow field inside the flotation element. When the intake hole is opened, extra air will be sucked into the chamber, where the original air rotates at a high speed. Then the vertical velocity of the air inside the chamber will increase because of the extra air. Finally, extra air will mix with the surrounding air and flow together into the gap.

Next, we discuss the velocity component and distribution of the XY plane inside the chamber. The respective horizontal cross-sections and vertical cross-sections of the flotation elements with and without an intake hole are captured, and presented in **Figure 8** and **Figure 9**, where color represents the amplitude $\sqrt{u_x^2 + u_y^2}$.

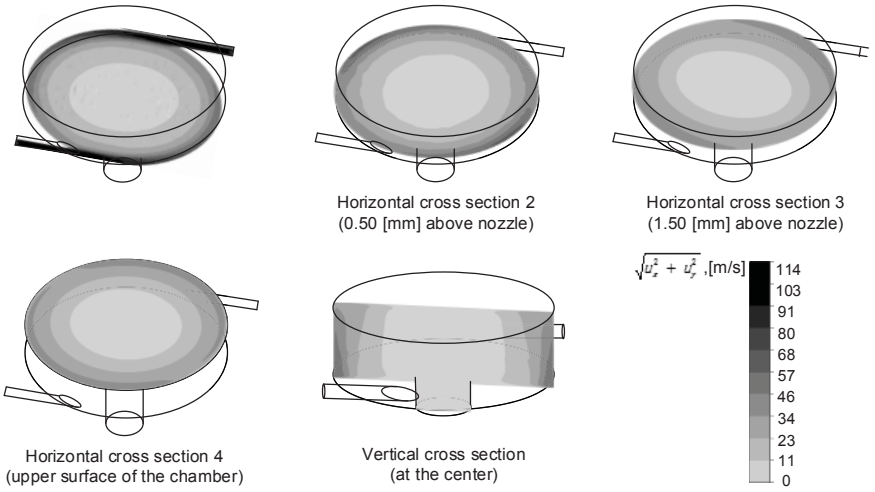

Figure 8: Velocity contour of flotation element without intake hole

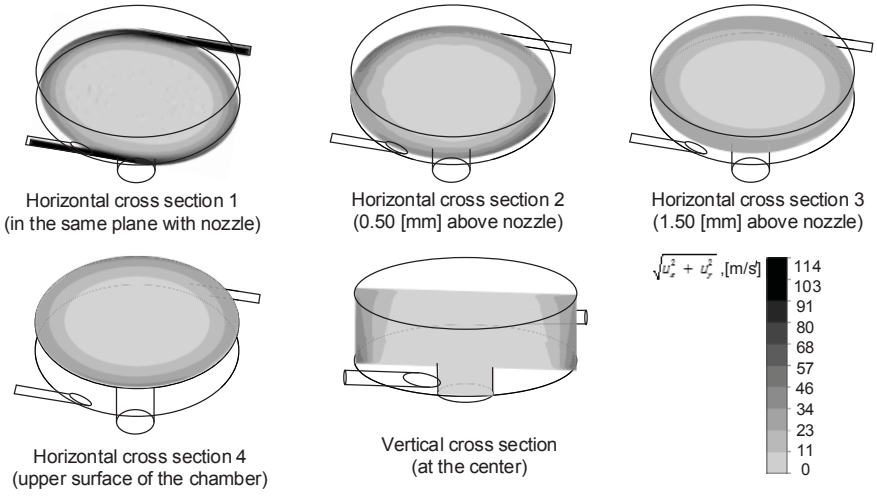

Figure 9: Velocity contour of flotation element with intake hole

We found that the velocity component of the flotation element without the intake hole is always higher. In other words, the horizontal rotational motion of air inside the flotation element with an intake hole is not as violent as that inside the flotation element without

an intake hole. This phenomenon can be explained from an energy perspective: the flotation element with an intake hole takes a part of the kinetic energy of the rotational flow to suck extra air, which results in the weakening of the horizontal rotation motion of air. This means the flotation element with an intake hole can take full advantage of the kinetic energy of air in the chamber and amplify the final output flow rate.

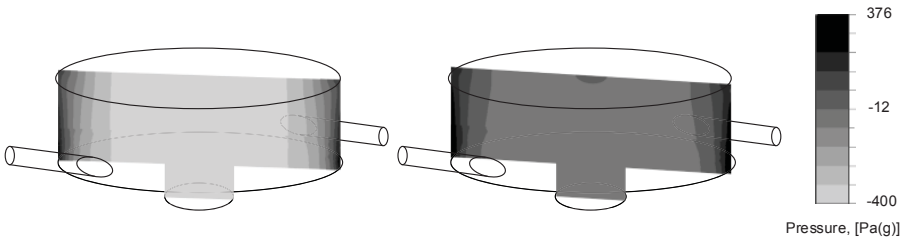

Figure 10: Pressure contour of vertical section plane (left: flotation element without intake hole, right: flotation element with intake hole)

The changes in the velocity field will significantly affect the pressure distribution inside the chamber. In order to learn about the connection between the intake hole and the pressure distribution inside the chamber, the pressure contours of two flotation elements are captured and presented in **Figure 10**. The chamber of the flotation element without an intake hole has a noticeable negative pressure region [the lowest pressure is approximately -400 Pa(g)]. The negative pressure region is less obvious in the chamber of the flotation element with an intake hole [the lowest pressure is only -50 Pa(g)]. As stated in the Introduction, the negative pressure region in the chamber is developed by a high-speed rotational flow. Once the intake hole is opened, the negative pressure developed by the high-speed rotational flow will decay to a value nearing the atmosphere pressure. In addition, the extra air has been accelerated since it was sucked into the chamber, and this will make the pressure of the chamber increase further if it is blocked by a workpiece surface. These factors lead to the negative pressure in the chamber of the flotation element with intake hole becoming less obvious.

3.3. Flow phenomenon in the gap

To explore the flow phenomenon in the gap, the pressure distribution along the radial direction of the flotation plane is necessary. It can be easily measured with the pressure measurement apparatus. The pressure distributions of the flotation elements with and the without an intake hole are presented in **Figure 11**. Both of them are measured with a supplied flow rate of 2 L/min(ARN) and a gap height of 0.25 mm.

The region between the dashed lines represents the area over the chamber, where the pressure is quite low in the flotation element without an intake hole and higher in the flotation element with an intake hole. This is the same as the condition inside the flotation element, which means the gap's pressure distribution over the chamber relates to the pressure distribution in the chamber.

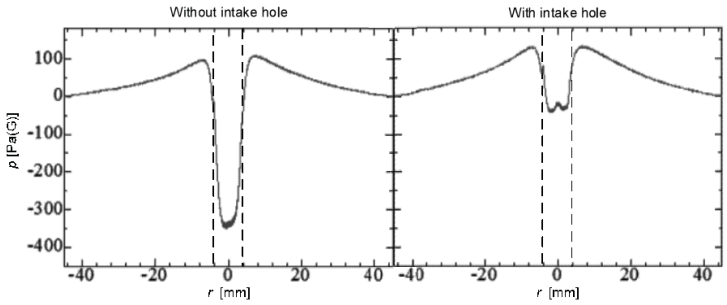

Figure 11: Pressure distribution in the gap between workpiece and flotation plane [supply flow rate Q = 2 L/min(ANR), height of gap h = 0.25 mm]

In the gap between the flotation plane and workpiece surface (the region outside of the dashed lines), the pressure of the flotation element with an intake hole is higher than that of the flotation element without an intake hole. This can be explained by the Navier-Stokes equations of gap flow. Set a cylinder system (r, α, z) at the flotation plane's centre, and make the following assumptions: (i) Airflow in the gap is laminar primarily because of the low Reynolds numbers of this case. (ii) The viscous effect is dominant in the very thin gap so that the inertia effect is negligible. (iii) Pressure distributions in the z and α directions are too small to be regarded. (iv) Neglect distributions in the r and α directions of velocities u_r and u_z. The radial pressure distribution in the gap can be donated by (1).

$$\frac{dp}{dr} = \frac{-\mu Q_{out}}{r\pi h^2} \tag{1}$$

where *h* is the gap height, and the values for both flotation elements are 0.25 mm. Q_{out} is the flow rate through the gap. For the flotation element without an intake hole, it equals the supplied flow rate, i.e. $Q''_{out} = Q''$, while it equals the supplied flow rate plus the intake flow rate for the flotation element with an intake hole, i.e. $Q'_{out} = Q' + Q'_{intake}$. Since the supplied flow rates Q' and Q'' are both 2 L/min(ARN), it is obvious that $Q'_{out} > Q''_{out}$ and the pressure distribution of the flotation element with an intake hole is higher than that of the flotation element without intake hole.

3.4. Influence of the gap height

The influences of the variant gap height are also discussed in this paper. The flotation plane pressure distribution along the radial direction of the flotation element in **Figure 12** is measured with a supplied flow rate of 2 L/min (ARN), where the dashed lines represent the edge of the chamber. The respective gap heights are 0.20 mm, 0.25 mm, 0.30 mm, 0.35 mm, and 0.40 mm.

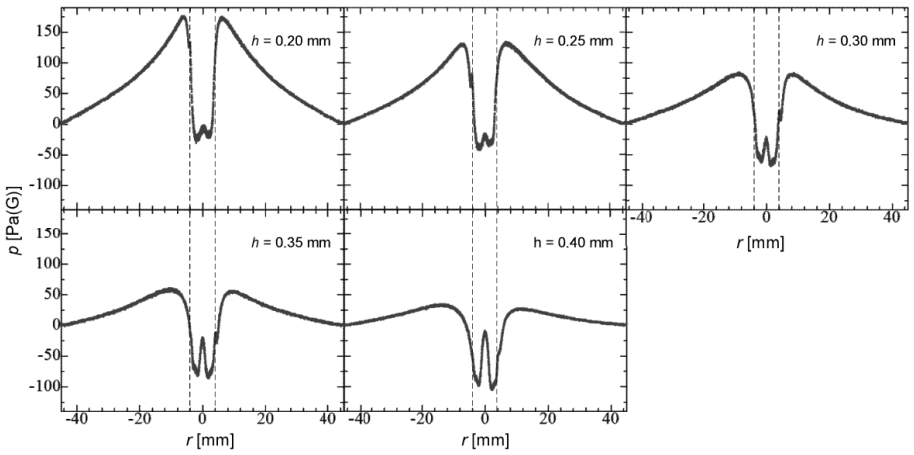

Figure 12: Pressure distribution in the gap between workpiece and flotation plane (supply flow rate Q = 2 L/min (ANR))

It is found that the region outside of the dashed lines is significantly affected by the gap height. Because it is dominated by the viscous effect, when the gap height increases, the viscous effect rapidly decays and the pressure distribution of this region decreases.

The pressure distribution between the dashed lines is related to the chamber. The same supplied flow rate produces the same pressure difference between the edge and the centre of the chamber. When the gap height increases, the pressure distribution outside of the dashed lines decreases. This results in a decrease in central pressure.

3.5. Influence of supplied flow rate

The changing supplied flow rate also affects the flow phenomenon in flotation element. Applying the pressure measurement apparatus, we obtained the flotation plane pressure distribution with different supplied flow rates, as shown in **Figure 13**. On comparing experimental results, it is found that the pressure distribution outside of the dashed lines increases as the supplied flow rate increases. When the supplied flow rate increases from 2 L/min(ARN) to 4 L/min(ARN), the highest pressure increases from 60

Pa(g) to 90 Pa(g) simultaneously. This is a positive correlation between the highest pressure and the supplied flow rate. The pressure distribution between the dashed lines is significantly affected by supplied flow rate. When the supplied flow rate is 2 L/min(ARN), the lowest pressure is -86 Pa(g). This decreases to -278 Pa(g) when the supplied flow rate is 4 L/min(ARN). As stated in the section 'Flow phenomenon in the gap', the pressure distribution between the dashed lines relates to the pressure distribution in the chamber. A higher supplied flow rate leads to a higher rotational speed and results in a lower negative pressure in the chamber. Because of the quadratic relation between the pressure difference developed by rotational flow and its velocity, a changing supplied flow rate will greatly influence the pressure in the chamber and reflect on the pressure distribution over the chamber in the end.

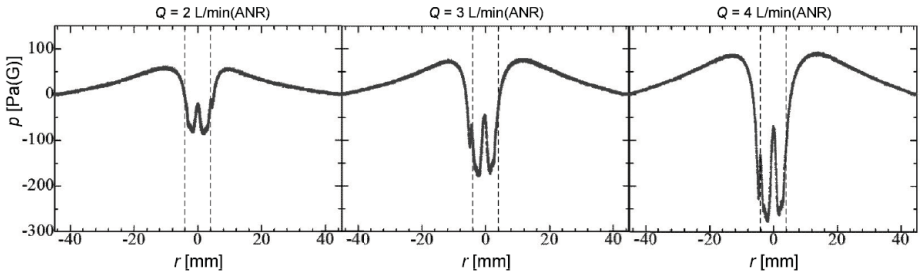

Figure 13: Pressure distribution in the gap between workpiece surface and flotation plane (gap height h = 0.25 mm)

4. Conclusions

Focusing on reducing the air consumption of an air flotation rail system, a new flotation element called as flowrate-amplified flotation element was recently proposed. To study the flow phenomenon in the flotation element, the pressure measurement apparatus and CFD simulations were designed and conducted to obtain overall fluid field data of flotation element.

In the present work, we discussed the inner flow phenomenon and pressure distribution in different situations. The influence of the intake hole, gap height, and supplied flow rate on the fluid field of the chamber and the gap were investigated. Our conclusions are as follows:

1. The flowrate-amplifier flotation element takes a part of the kinetic energy of the rotational flow to suck in extra air and amplify the flow rate.
2. Extra air is sucked into the chamber through an intake hole and mixes with supplied air in the end. Extra air will improve the pressure in the gap.

3. The pressure distribution of the gap is dominated by a viscous effect. It will decreases as the gap height increases and the viscous effect decays. The pressure difference between the edge and the centre of the chamber is dominated by inertia. The gap height has little effects on it.
4. As the supplied flow rate increases, the air in the chamber rotates more rapidly and develops a lower negative pressure. The flow rate through the gap also increases, which results in an increase in the pressure distribution of the gap.

5. References

/1/ N. Oiwa, M. Masuda, T. Hirayama, T. Matsuoka, and H. Yabe, "Deformation and flying height orbit of glass sheets on aerostatic porous bearing guides," *Tribology International,* vol. 48, pp. 2-7, 2012.

/2/ K. Amano, S. Yoshimoto, M. Miyatake, and T. Hirayama, "Basic investigation of noncontact transportation system for large TFT-LCD glass sheet used in CCD inspection section," *Precision Engineering,* vol. 35, pp. 58-64, 2011.

/3/ R. Adin and Y. Yassour, "56.2: Contactless LCD Fab: From Technology to Implementation," in *SID Symposium Digest of Technical Papers*, pp. 1492-1495, 2004.

/4/ A. Delettre, G. J. Laurent, and L. Fort-Piat, "A new contactless conveyor system for handling clean and delicate products using induced air flows," in *Intelligent Robots and Systems (IROS), 2010 IEEE/RSJ International Conference on*, pp. 2351-2356, 2010.

/5/ H. G. Lee, "Design of a large LCD panel handling air conveyor with minimum air consumption," *Mechanism and machine theory,* vol. 41, pp. 790-806, 2006.

/6/ X. Li, Z. Guo, and T. Kagawa, "Development and experimental evaluation of air flotation element with additional air-intake capacity," *Lubrication Science,* 2015.